




**Inhomogeneity effects on earthquake fault events**S. Tahir <sup>\*</sup>, M. Loulidi <sup>†</sup> and A. Rachadi*Laboratory of Condensed Matter and Interdisciplinary Sciences, Unite de Recherche Labellisee CNRST, URL-CNRST-17, Faculty of Sciences, Mohammed V University of Rabat, Rabat 1014, Morocco* (Received 16 January 2024; accepted 15 August 2024; published 10 September 2024)

We present a detailed analysis of the dynamical behavior of an inhomogeneous Burridge-Knopoff model, a simplified mechanical model of an earthquake. Regardless of the size of seismic faults, a soil element rarely has a continuous appearance. Instead, their surfaces have complex structures. Thus, the model we suggest keeps the full Newtonian dynamics with inertial effects of the original model, while incorporating the inhomogeneities of seismic fault surfaces in stick-slip friction force that depends on the local structure of the contact surfaces as shown in recent experiments. The numerical results of the proposed model show that the cluster size and the moment distributions of earthquake events are in agreement with the Gutenberg-Richter law without introducing any relaxation mechanism. The exponent of the power-law size distribution we obtain falls within a realistic range of value without fine tuning any parameter. On the other hand, we show that the size distribution of both localized and delocalized events obeys a power law in contrast to the homogeneous case. Thus, no crossover behavior between small and large events occurs.

DOI: [10.1103/PhysRevE.110.034206](https://doi.org/10.1103/PhysRevE.110.034206)**I. INTRODUCTION**

Earthquakes are among systems in nature whose dynamics present self-organized critical behavior which results from large critical fluctuations since such systems are in a perpetual critical steady state. Driven at a critical threshold of instability, they trigger events of a wide range of sizes that follow a power-law behavior [1].

Earthquake faults result from the fact that the surface of two moving tectonic plates, when they come in contact with each other, is imperatively driven toward a slipping instability, triggering events of different magnitudes  $m$  that are distributed according to the Gutenberg-Richter (GR) law [2], which states that the number of earthquakes of magnitude greater than or equal to  $m$  is given by

$$\log_{10} N(m) = a - Bm, \quad (1)$$

where  $a$  and  $B$  are positive parameters that differ from one region to another, and generally  $B$  is in the range  $0.6 \leq B \leq 1.3$  [3,4].

The Burridge-Knopoff (BK) model is the simplest continuum model that may describe qualitatively the mean characteristics of the earthquake faults. It has been intensively studied numerically in one dimension [5–10]. Carlson and Langer showed that the model exhibits three kinds of sleeping events, namely the smallest ones involving motions

at small length scale, large localized events, and delocalized great events [6]. The moment distribution of localized events  $P(M) \sim M^{-b}$  is consistent with the GR law with  $b \approx 2$ , especially for high values of the weakening velocity parameter on which the friction force depends. The moment distribution of the delocalized event does not present any power-law behavior. On the other hand, Xia and co-workers [10] have studied numerically the BK model in one dimension, and their results show that the cluster size distribution  $n(s)$  for large events depends on the time step and there is a small range of  $s$  that poorly exhibits power-law scaling with exponent  $b \approx 2.5$ . Assuming a long stress transfer, Xia *et al.* [9] showed that the statistical properties are different from the original BK model and they depend either on the range of the stress and the friction force characteristics. Inspired by the BK model and the idea of self-organized criticality, different nonconservative self-organized critical models have been elaborated based on cellular automaton (CA) rules [11–13]. Such models were able to reproduce the power-law behavior but the scaling-law exponent depends strongly on the elastic parameter  $\alpha$  and the real exponent is obtained only around  $\alpha = 0.2$ . We point out that a robust scaling law was observed only when an internal relaxation process has been incorporated [13].

In reality, the friction law depends on the composition of fault rocks, which rarely have a homogeneous appearance [14–19]. Thus, in the present paper, we suggest a more realistic BK model by taking into account the inhomogeneities located at the surface of the tectonic plates. Such inhomogeneities have a relevant impact on the friction force which leads to different statistical properties of different events. Thus, in Sec. II, the inhomogeneous BK model we suggest and its associated parameters are presented. A theoretical analysis of the inhomogeneity effect on the three categories of events is provided in Sec. III. The results of our numerical simulations which include the cluster size and the moment cumulative distributions are presented in Sec. IV. Finally, Sec. V is

<sup>\*</sup>Contact author: [saida\\_tahir@um5.ac.ma](mailto:saida_tahir@um5.ac.ma);  
[tahirsaida1995@gmail.com](mailto:tahirsaida1995@gmail.com)

<sup>†</sup>Contact author: [loulidim60@gmail.com](mailto:loulidim60@gmail.com)

dedicated to the conclusion where a brief summary of the main results is given.

## II. DEFINITION OF THE MODEL AND ITS MAIN CHARACTERISTICS

As in the original model [20], the system we consider consists of a chain of  $N$  blocks of mass  $m$  joined to each other by springs of strength  $k_S$  and linked to a fixed plate by leaf springs of strength  $k_L$ . The blocks are in contact with a surface which moves at relative velocity  $v$  causing a velocity-weakening stick-slip friction force that is the origin of the system instability. Unlike the version of the BK model where the system is uniform with no spatial parameters, variations, or stochastic elements [6], we introduce a friction force that depends locally on the structure of the substrate.

The equations of motion of the model are given by

$$m\ddot{x}_j = k_S(x_{j+1} - 2x_j + x_{j-1}) - k_L x_j - F(v + \dot{x}_j), \quad (2)$$

where  $x_j$  is the displacement of block  $j$  ( $j = 1, 2, \dots, N$ ) relative to its equilibrium position and the friction law  $F$  is assumed to be of the form

$$F(\dot{x}) = F_r \phi(\dot{x}/\bar{v}), \quad (3)$$

where  $\phi$  is a vanishing function,

$$\phi(y) = \frac{\text{sgn}(y)}{1 + |y|}, \quad (4)$$

$F_r$  is a random amplitude of mean  $\mathbb{E}(F_r) = F_0$  and variance  $\text{var}(F_r) = \sigma^2$  that follows a Gaussian distribution law, and  $\bar{v}$  is the velocity dependence of  $F$  at which the friction is considerably reduced. After an appropriate rescaling,

$$\tau = \omega_p t, \quad u_j = D_0 x_j, \quad (5)$$

where  $\omega_p = \sqrt{k_L/m}$  is the period of a moving single block in the absence of friction and  $D_0 = F_0/k_L$  presents the maximum averaged displacement before slipping, Eq. (2) is rewritten in the scaled form,

$$\ddot{u}_j = l^2(u_{j+1} - 2u_j + u_{j-1}) - u_j - \eta_j \phi(2\alpha v + 2\alpha \dot{u}_j), \quad (6)$$

where

$$l^2 = k_S/k_L, \quad v = \bar{v}/(\omega_p D_0), \quad 2\alpha = \omega_p D_0/\bar{v}, \quad (7)$$

are the parameters that govern the system dynamics, and  $\eta = \frac{F_r}{F_0}$  is a random variable with mean  $\mathbb{E}(\eta) = 1$  and variance  $\sigma'^2 = \frac{\sigma^2}{F_0^2}$ . As it was pointed out by Carlson and Langer [6], the delocalized large events happen when the slipping time, i.e.,  $\omega_p^{-1}$ , is very small compared to the loading time, i.e.,  $D_0/v$ . Thus, the dynamics of such an event should be analyzed in the continuum limit where the spacing blocks  $a$  are small enough ( $a \rightarrow 0$ ). Defining new length dimension variables  $s = ja$  and  $\xi = \ell a$ , Eq. (6) is rewritten as

$$\ddot{u} = \xi^2 \frac{\partial^2 u}{\partial s^2} - u - \eta \phi(2\alpha v + 2\alpha \dot{u}). \quad (8)$$

Following the wave propagation equation,  $\xi$  is viewed as a sound speed. Since for small events, called microscopic events, few blocks are displaced and the variation of their displacement  $u_j$  is small, the spacing  $a$  between blocks remains

fixed. Consequently, to study the dynamics of such events we have to consider Eq. (6) in its discrete form.

## III. INHOMOGENEITY EFFECTS ON DIFFERENT EVENTS

As mentioned above, the events are divided into microscopic, localized, and delocalized depending on the parameter  $v$ , the ratio of the slipping time, and the loading time. The microscopic events consist of a few connected blocks that slip as a whole between stuck blocks on either side. By shifting to a frame of reference whose origin is the center of mass of the group of  $n$  blocks and following the analysis of Carlson and Langer [6], the motion equation of the displacement  $W_n$  in the new frame of reference is

$$\ddot{W}_n = -\Omega_n^2 W_n + v\tau + 1 - \frac{1}{n} \sum_j \eta_j \phi(2\alpha \dot{W}_n), \quad (9)$$

with the initial conditions  $W_n = \dot{W}_n = 0$  for  $\tau = 0$ . Equation (9) is the same as the one of the homogeneous models [6] with a friction term that may be considered as an average on the different blocks' friction inhomogeneity represented by the stochastic parameter  $\eta_j$ . For small events, the variation of the displacements  $u_j$  is very small and so  $\dot{W}_n$  is small enough to allow the linearization of  $\Phi$  by assuming that  $2\alpha \dot{W}_n$  is small. Then Eq. (9) can be rewritten for small  $n$  as

$$\ddot{W}_n - 2\tilde{\alpha} \dot{W}_n + \Omega_n^2 W_n \cong v\tau + 1 - \tilde{\eta}, \quad (10)$$

with

$$\tilde{\alpha} = \frac{\alpha}{n} \sum_j \eta_j, \quad \text{and} \quad \tilde{\eta} = \frac{1}{n} \sum_j \eta_j. \quad (11)$$

Since for small  $n$ ,  $\tilde{\alpha}$  is small enough that  $\tilde{\alpha} \ll \Omega_n$ , then the solution of Eq. (10) [given in the Supplemental Material, Eq. (S1) [21]] becomes

$$W_n(\tau, \tilde{\eta}) = \frac{v}{\Omega_n^2} \left[ \tau - \frac{\sin(\tau \Omega_n)}{\Omega_n} \right] + \frac{(\tilde{\eta} - 1)}{\Omega_n^2} [\cos(\tau \Omega_n) - 1]. \quad (12)$$

Equation (12) contains two contributions. The first one is none other than the solution of the homogeneous model [6], which we find for  $\tilde{\eta} = 1$ , while the second contribution results from inhomogeneities. Averaging over such inhomogeneities that are distributed according to a Gaussian distribution law of mean  $\mu$  and standard deviation  $\sigma$ , we obtained

$$W_n(\tau) = \frac{v}{\Omega_n^2} \left[ \tau - \frac{\sin(\Omega_n \tau)}{\Omega_n} \right] - \frac{\frac{\sigma}{\sqrt{2\pi}} e^{-\frac{\mu^2}{2\sigma^2}} - \frac{\mu}{2} [1 + \text{erf}(\frac{\mu}{\sigma\sqrt{2}})] + 1}{\Omega_n^2} [\cos(\Omega_n \tau) - 1]. \quad (13)$$

We note that the solution of the homogeneous model is found for  $\mu = 1$  and  $\sigma = 0$ , where the second term of Eq. (13) vanishes. The distance that the group of blocks travels during a time interval  $\delta\tau = 2\pi/\Omega_n$  before coming to rest is

$$\delta W_n = \frac{2\pi v}{\Omega_n^3}, \quad (14)$$

and the average speed is given by

$$\frac{\delta W_n}{\delta \tau} = \frac{\nu}{\Omega_n^2} \equiv \frac{n\nu}{2l^2}. \quad (15)$$

We remark that the average displacement  $W_n$  in Eq. (13) depends on the inhomogeneity distribution while the average speed of the  $n$  blocks in Eq. (15) does not depend on it. This is due to the fact that for a small group of blocks undergoing small periodic events with brief sticks, the contribution of the average friction oscillates along this period of time  $\delta\tau$  leading to a vanishing contribution of its variation.

The localized and delocalized events are described in the continuum limit rather than the discrete version of the equation of motion. Writing  $u(s, \tau) = u_\epsilon(s) + u(s, \tau)$  [6] where  $u_\epsilon(s)$  is the solution of a stationary state that corresponds to a balance between coupling, pulling forces, and the maximum of the friction force, and assuming that  $\dot{u} \gg \nu$ , the system dynamical equation that we have to solve is

$$\ddot{u} - \xi^2 \frac{\partial^2 u}{\partial s^2} + u = 1 - \eta(s)\phi(2\alpha\nu + 2\alpha\dot{u}) \cong 1 - \eta(s)(1 + 2\alpha\dot{u}), \quad (16)$$

with the initial conditions

$$u(s, 0) = 0, \quad \dot{u}(s, 0) = \omega_0 \delta(s - s_0), \quad (17)$$

where  $s_0$  is the position of the initial triggered slipping event generated by simultaneous small pulses and  $\omega_0$ , which is proportional to  $\nu$ , is the slipping speed of such events [6]. After laborious calculations (see some steps in Supplemental Material Sec. S2 [21]), the solution we find,

$$\dot{u}(s, \eta, \tau) = \frac{1}{2}\omega_0 e^{\tilde{\alpha}\tau} [\delta(s - s_0 + \xi\tau) + \delta(s - s_0 - \xi\tau)], \quad (18)$$

is analogous to the one of the homogeneous model [6], except that  $\tilde{\alpha}$  is a random parameter that is distributed according to a Gaussian law leading to a random exponential growth of the velocity pulses. Averaging over the disorder of friction force we obtain

$$\dot{u}(s, \tau) = \frac{1}{4}\omega_0 e^{\alpha\tau + \frac{(\sigma\alpha\tau)^2}{2}} \left[ \operatorname{erf}\left(\frac{\sigma^2\alpha\tau + \mu}{\sigma\sqrt{2}}\right) + 1 \right] \times [\delta(s - s_0 + \xi\tau) + \delta(s - s_0 - \xi\tau)], \quad (19)$$

which consists of the propagation of advanced and retarded waves away from the source point  $s_0$  at the sound speed  $\xi$ . We note that even if the solution of the system dynamical Eq. (19) is qualitatively similar to the one of the homogeneous case, the amplitude of the pulse velocities is larger than the one of the uniform system. As a result,  $\phi$  decreases and the effect of frictional instabilities increases considerably the amplification of the spatial irregularities, leading to an increase of the slipping zone. Thus, the average size of the localized events becomes larger than the one of the homogeneous model. Such a case is depicted in Figs. S1(a) and S1(b) [21]. The increase of the localized event size may dislodge blocks located at the neighbor of the initial slipping zone, which may lead to the appearance of relatively large localized events. As a consequence, the power law of the size and the moment distributions will be quantitatively improved as we will see in the numerical simulations discussed in Sec. IV.

On the other hand, the delocalized events result from the fact that the pulses grow enough to dislodge blocks far from the initially slipping zone. One can see from Eq. (19) that the ratio between velocity amplitudes of the inhomogeneous and homogeneous cases denoted  $R_{\dot{u}}$  is  $1 < R_{\dot{u}} < 2e^{\frac{\alpha\tau\sigma^2}{2}}$ . Thus, the pulses will overflow the slipping zone more than in the homogeneous case. As a result, the average size of delocalized events will be greater than the one of a uniform system and their frequency will increase, which will have an impact on the size and moment distributions of these large events that will exhibit a power-law distribution (see Sec. IV), unlike the homogeneous case where the distribution of large events does not present a such behavior [6] [Figs. S1(c) and S1(d) [21]].

#### IV. NUMERICAL RESULTS

The system dynamical Eq. (6) is solved numerically for different values of  $\alpha$ ,  $\nu$ , and  $\ell$  with system size  $N = 1500$  and open boundary conditions, i.e., the end blocks of the chain are stuck, to discard any finite-size effect.

The events that mostly occur in the BK model are slipping as a cluster of blocks. These are divided into “stuck” or “slipped,” namely that the block is considered stuck if its speed is less than a parameter  $\nu_0$ . A random amplitude of the friction force is assigned to each block according to a Gaussian distribution whose mean and variance are  $\mu$  and  $\sigma$ , respectively. Note that the friction force is renewed after each slip event. We initially started the system in a full stuck configuration with small random displacements to all blocks. Finally, we accumulate data after the system reaches ten loading periods  $\frac{2}{\nu}$ . After reaching a steady state, the system presents a variety of different events with different sizes. The numerical data we obtained have been analyzed in terms of event size  $s$ , the number of connected blocks that move during an event, and the moment  $M$ , which is the analogous measure of a seismic event size. It depends on the net displacement of block  $i$ ,  $\delta u_i$ , defined as follows,

$$M = \sum_i \delta u_i, \quad (20)$$

where the sum is seized from all the blocks moving during the event. In order to estimate correctly the exponent of the power-law behavior of the moment distribution, we use the moment cumulative distribution  $\mathcal{P}(M)$  to eliminate fluctuations. Following an analysis of measuring power laws [22], it has been shown that the cumulative distribution follows the same power-law behavior as the one of the original distribution, but with an exponent  $\beta = b - 1$ .

The cluster size distribution and the moment distribution with various values of  $\sigma$  and  $\alpha$ , for  $\ell = 10$ ,  $\nu = 0.01$ , and  $N = 1500$ , are represented in Figs. 1 and 2. As shown analytically, the average velocity of small events does not depend on the friction force randomness [Eq. (15)]. Such a result is in good agreement with the obtained numerical results (see Figs. 1 and 2) since the moment and the size distributions for the small event do not depend on the randomness character. We remark that both localized and delocalized events exhibit a power-law behavior for all values of  $\alpha \neq 0$  and  $\sigma \neq 0$ . The distributions of the homogeneous system are found for

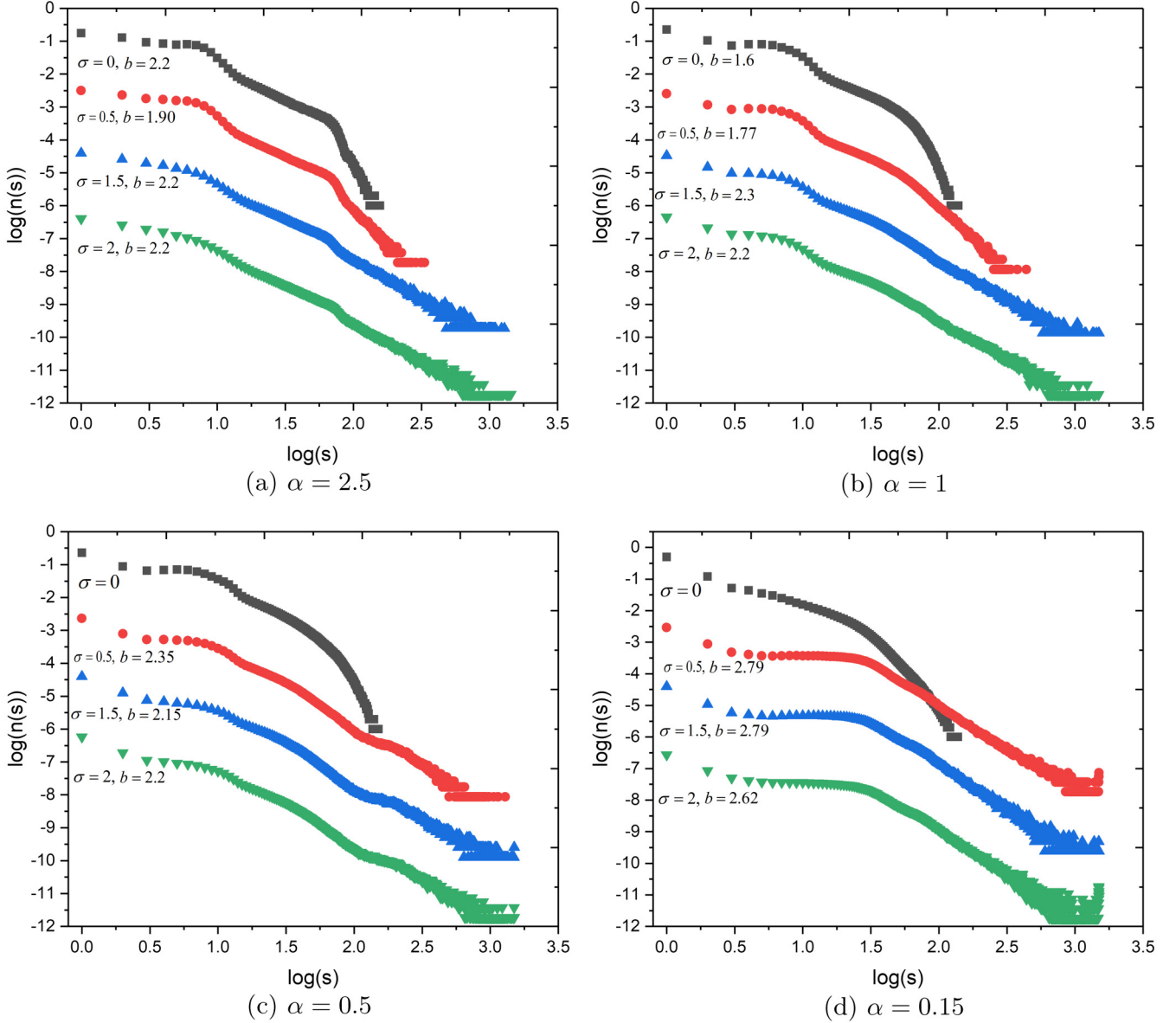


FIG. 1. The cluster size distribution  $n(s)$  as a function of  $s$  for different values of  $\sigma$  and  $\alpha$ . All plots have been relocated vertically to ensure clarity.

$\sigma = 0$  and they do not present any power-law behavior for  $\alpha < 1$ , which is consistent with those in Ref. [6] and shown numerically in Refs. [9,10]. The simulation results show that for low values of the standard deviation  $\sigma \ll 1$  and  $\alpha > 1$ , there is two regions corresponding to localized and delocalized events that both present a power-law behavior but with different exponents as shown in Figs. 1(a) and 1(b). Such a result reveals that the crossover between those events still remains as in the homogeneous case [6] but with identical behavior for both events, unlike the homogeneous case where a pronounced peak was observed in the delocalized event distribution [6]. Thus, a small amount of heterogeneity allows for the restoration of the power-law behavior for delocalized large events. For  $\sigma > 1$  both event distributions present the same exponent  $b$ .

Assuming that there exists a limit moment  $M_l$  that delimits the scaling region, we may show that such a limit is rejected to

infinity in the BK model with heterogeneous friction. Indeed, as it was defined by Carlson and Langer [6],  $M_l$  is given by

$$M_l = 2 \int_0^{\xi_l/2} \delta U(\Delta s) d(\Delta s), \quad (21)$$

where  $\xi_l = 2\Delta s$  is the length of the unstable localized slipping region. After some calculations using Eq. (17) (see Sec. S3 of the Supplemental Material [21]), we get

$$M_l \simeq \frac{2va}{4\alpha\ell^2} e^{\frac{\alpha}{2\xi}\xi_l} + \frac{\sigma^2}{16\alpha} e^{3\alpha\frac{\xi_l}{v\ell}}. \quad (22)$$

After a development of the ratio  $\xi_l/\xi$ , we obtain

$$M_l \simeq \frac{2\xi}{\alpha} + \frac{\sigma^2}{16\alpha} \left( \frac{6\xi}{va} \right)^6. \quad (23)$$

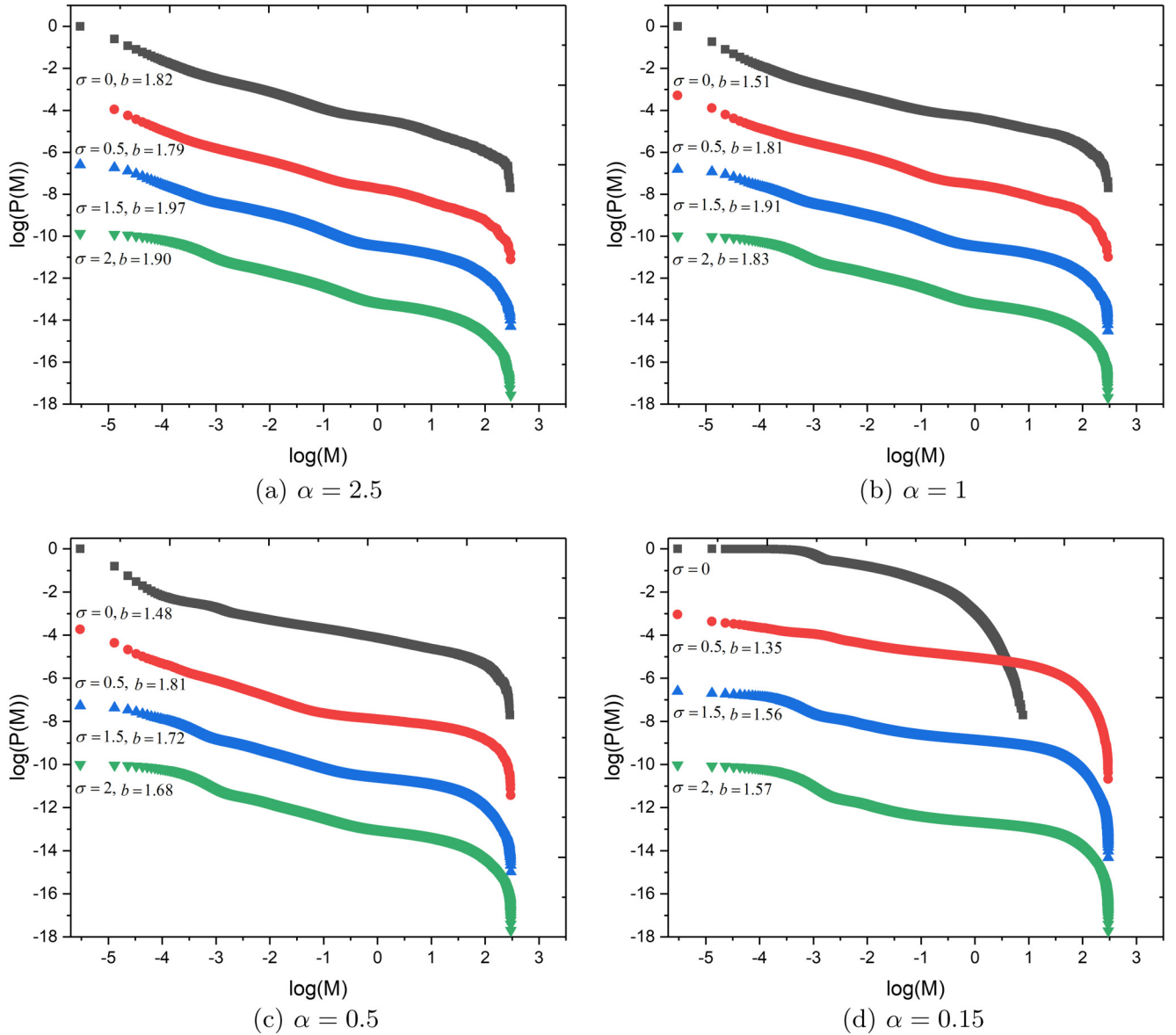


FIG. 2. The cumulative distribution of the moment  $\mathcal{P}(M)$  as a function of  $M$  for different values of  $\sigma$  and  $\alpha$ . All plots have been relocated vertically to ensure clarity.

The first term in Eq. (23) is the  $M_l$  of the homogeneous model. The last term, which is of order  $O\{\{\xi/(\nu a)\}^6\}$ , is so wide that it discards the limit moment to infinity.

The crossover observed in the size distribution cannot be clearly identified in the moment distribution because two different events with different sizes may have the same moment. Thus, the moment associated with both events exhibits a power-law behavior with the same exponent  $b$  (Fig. 2) for all values of  $\sigma$  except for low values of  $\alpha$  where the scaling region is not accurately defined for  $\sigma = 0$  and large values of  $\sigma$  in Fig. 2(d). The size distribution power-law exponent we found is in agreement with the one of the GR law  $b \sim 2$  for all values of  $\sigma$  and  $\alpha > 1$  while it exhibits larger values for small standard deviations and relatively lower values of  $\alpha$  [Fig. 1(c)]. For very low values of  $\alpha$ , the scaling region of the size distribution is relatively reduced since this one presents

a small region of medium events that are almost equally distributed and the localized and delocalized events exhibit a power-law distribution where the exponent is greater than the GR exponent,  $b \sim 2.7$ . We note that in our model, the scaling law is maintained even if the largest slipping speed is less than the speed  $\bar{v}$ , i.e.,  $\alpha < 1$ , which characterizes the velocity dependence of the friction force. Since the heterogeneity of the friction force prevents the localized events to be extended and run into each other as what happens for the uniform system [6], the frequency of localized events will increase, leading to a power-law distribution rather than a quasiuniform distribution observed for homogeneous friction force [6]. It is worthwhile to note that the obtained results in Figs. 1 and 2 are in agreement with the results of a recent experimental study of laterally heterogeneous faults [23] for which the failure strength and stability of experimental faults are reduced

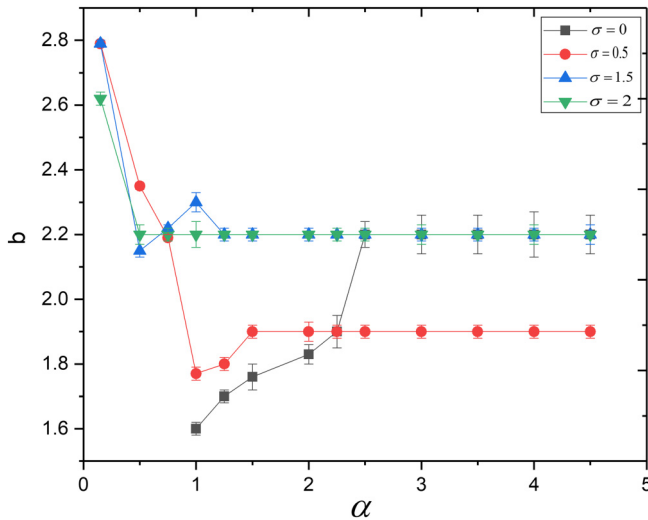


FIG. 3.  $b$  vs  $\alpha$  for different values of  $\sigma$ .

significantly compared to identical but homogeneous mixed gouges, by introducing simple heterogeneous structures into the fault zone. Consequently, that affects the slipping speed of the blocks and then new events will appear. Thus, the sizes of the events will increase and so will the scaling range. On the other hand, Carlson and Langer [6] have performed numerical simulations on a system of size  $N = 100$ , and the exponent  $B$  of the GR power law they obtain for the homogeneous model ( $\sigma = 0$ ) is slightly different from the one we obtained. Such a difference may result from the fact that the exponent  $B$  depends on the fault region and the finite-size effects [4].

The variation of the size distribution exponent  $b$  vs  $\alpha$  is shown in Fig. 3. Compared to the homogeneous model ( $\sigma = 0$ ), it is clear that the range of the parameter  $\alpha$  where the exponent is constant and in excellent agreement with the GR law is enlarged for different values of  $\sigma$ . As mentioned above, such a result is due to the fact that the size of localized events may not extend for a nonuniform system as it was shown experimentally [23] and the statistics of medium events will increase as new localized events are triggered. Opposite to the homogeneous model, the scaling law persists even for low values of  $\alpha < 1$ , and the corresponding exponents differ more or less from the GR law exponent depending on the standard deviation of inhomogeneities (see Fig. 3).

## V. CONCLUSION

Since real earthquake faults present different irregularities, especially a nonuniform friction force at the fault surface, we presented a detailed analysis of spatial inhomogeneity effects on the different events by considering the simple Burridge-Knopoff model with a stochastic friction force. The dynamical equations of microscopic, localized, and delocalized events have been studied analytically to illustrate the effects of friction force inhomogeneities on their propagating motions. Numerical simulations showed that the size and the moment distributions are in good agreement with the GR law for both localized and large delocalized events for all values of the model parameter  $\alpha$ , in contrast to the homogeneous case where the size distribution of delocalized events is not part of the scaling region. We showed that depending on the parameter  $\alpha$ , the region where the exponent of the moment distribution agrees with the one of the GR law is enlarged. On the other hand, even for very low values of  $\alpha$ , the scaled law is maintained with relatively higher values of the corresponding exponent. Such a result is in agreement with what was found using a rigorous mathematical analysis of the experimental catalogs where it was shown that the GR law exponent is not constant and depends on the fault region [4]. Following the obtained results and the numerical analysis we performed (Fig. S1 [21]), it is worthwhile to mention that it seems that the inhomogeneous model we suggest may exhibit some kind of temporal clustering before and after the main shock, as it was observed in Fig. S1 [21]. However, it will be interesting to see if the model exhibits a sequence of foreshocks and aftershocks without introducing any relaxation mechanism [24]. Despite those results, improvements remain to make the model more realistic, because real earthquake faults are two-dimensional (2D) rather than one-dimensional systems. The two-dimensional BK model has already been studied by Mori and Kawamura [25,26]; they found that the exponent of the GR power law depends on the parameter  $\alpha$ , so it is desirable to study the 2D version of the model with the introduction of the heterogeneity in a future work.

## ACKNOWLEDGMENTS

This research was supported by computational resources of HPC-MARWAN [27] provided by the National Center for Scientific and Technical Research (CNRST), Rabat, Morocco.

- [1] D. L. Turcotte, *Fractals and Chaos in Geology and Geophysics* (Cambridge University Press, Cambridge, UK, 1997).
- [2] B. Gutenberg and C. F. Richter, Earthquake magnitude, intensity, energy, and acceleration: (Second paper), *Bull. Seismol. Soc. Am.* **46**, 105 (1956).
- [3] P. A. Varotsos, N. V. Sarlis, E. S. Skordas, and H. Tanaka, A plausible explanation of the  $b$ -value in the Gutenberg-Richter law from first principles, *Proc. Jpn. Acad., Ser. B* **80**, 429 (2004).
- [4] C. Godano, E. Lippiello, and L. de Arcangelis, Variability of the  $b$  value in the Gutenberg-Richter distribution, *Geophys. J. Int.* **199**, 1765 (2014).
- [5] J. M. Carlson and J. S. Langer, Properties of earthquakes generated by fault dynamics, *Phys. Rev. Lett.* **62**, 2632 (1989).
- [6] J. M. Carlson and J. S. Langer, Mechanical model of an earthquake fault, *Phys. Rev. A* **40**, 6470 (1989).
- [7] J. M. Carlson, J. S. Langer, B. E. Shaw, and C. Tang, Intrinsic properties of a Burridge-Knopoff model of an earthquake fault, *Phys. Rev. A* **44**, 884 (1991).
- [8] T. Mori and H. Kawamura, Simulation study of spatiotemporal correlations of earthquakes as a stick-slip frictional instability, *Phys. Rev. Lett.* **94**, 058501 (2005).
- [9] J. Xia, H. Gould, W. Klein, and J. B. Rundle, Simulation of the Burridge-Knopoff model of earthquakes with

- variable range stress transfer, *Phys. Rev. Lett.* **95**, 248501 (2005).
- [10] J. Xia, H. Gould, and W. Klein, Simulations of the Burridge-Knopoff model, in *3rd APEC Cooperation for Earthquake Simulation (ACES) Workshop, Maui, Hawaii, USA, 2002*, edited by A. Donnellan and P. Mora (APEC Cooperation for Earthquake Simulation, University of Queensland, Brisbane, 2003).
- [11] Z. Olami, H. J. S. Feder, and K. Christensen, Self-organized criticality in a continuous, nonconservative cellular automaton modeling earthquakes, *Phys. Rev. Lett.* **68**, 1244 (1992).
- [12] E. Jagla, Realistic spatial and temporal earthquake distributions in a modified Olami-Feder-Christensen model, *Phys. Rev. E* **81**, 046117 (2010).
- [13] E. Jagla and A. Kolton, A mechanism for spatial and temporal earthquake clustering, *J. Geophys. Res.* **115**, 2009JB006974 (2010).
- [14] C. Collettini, A. Niemeijer, C. Viti, and C. Marone, Fault zone fabric and fault weakness, *Nature (London)* **462**, 907 (2009).
- [15] J. G. Solum, N. C. Davatzes, and D. A. Lockner, Fault-related clay authigenesis along the Moab Fault: Implications for calculations of fault rock composition and mechanical and hydrologic fault zone properties, *J. Struct. Geol.* **32**, 1899 (2010).
- [16] C. Morrow, J. Solum, S. Tembe, D. Lockner, and T.-F. Wong, Using drill cutting separates to estimate the strength of narrow shear zones at SAFOD, *Geophys. Res. Lett.* **34**, 2007GL029665 (2007).
- [17] J. H. Dieterich, Modeling of rock friction: 1. Experimental results and constitutive equations, *J. Geophys. Res.* **84**, 2161 (1979).
- [18] A. Ruina, Slip instability and state variable friction laws, *J. Geophys. Res.* **88**, 10359 (1983).
- [19] L. de Arcangelis, C. Godano, J. R. Grasso, and E. Lippiello, Statistical physics approach to earthquake occurrence and forecasting, *Phys. Rep.* **628**, 1 (2016).
- [20] R. Burridge and L. Knopoff, Model and theoretical seismicity, *Bull. Seismol. Soc. Am.* **57**, 341 (1967).
- [21] See Supplemental Material at <http://link.aps.org/supplemental/10.1103/PhysRevE.110.034206> for the solution of the equation of the motion for the small event (Sec. S1), the solution of the equation of the motion for the localized and delocalized events (Sec. S2), the calculation of the limit moment (Sec. S3), and the delocalized and localized event for the homogeneous and inhomogeneous cases (Fig. S1).
- [22] M. E. J. Newman, Power laws, Pareto distributions and Zipf's law, *Contemp. Phys.* **46**, 323 (2005).
- [23] J. D. Bedford, D. R. Faulkner, and N. Lapusta, Fault rock heterogeneity can produce fault weakness and reduce fault stability, *Nat. Commun.* **13**, 326 (2022).
- [24] S. Tahir and M. Loulidi (unpublished).
- [25] T. Mori and H. Kawamura, Simulation study of the two-dimensional Burridge-Knopoff model of earthquakes, *J. Geophys. Res.: Solid Earth* **113**, B06301 (2008).
- [26] T. Mori and H. Kawamura, Simulation study of earthquakes based on the two-dimensional Burridge-Knopoff model with long-range interactions, *Phys. Rev. E* **77**, 051123 (2008).
- [27] [www.marwan.ma](http://www.marwan.ma).